JOURNAL OF SOLID STATE CHEMISTRY 119, 98–106 (1995)

Preparation of Cubic Niobium Pyrophosphate Containing Nb(IV) and Topotactic Extraction of Phosphorus Atoms

Hiroshi Fukuoka, Hideo Imoto, and Taro Saito

Department of Chemistry, School of Science, The University of Tokyo, Hongo, Bunkyo-ku, Tokyo 113, Japan

Received December 30, 1994; in revised form April 20, 1995; accepted April 24, 1995

A reduced phase of niobium pyrophosphate containing Nb^{4+} has been prepared from the reaction of $Nb_6Cl_{14} \cdot 8H_2O$ and phosphoric acid. The X-ray powder diffraction and electron diffraction studies have shown that the compound belongs to the $Pa\bar{3}$ space group and has the ZrP_2O_7 structure with a cubic superstructure ($a' = 3a_0$). Magnetic susceptibility was measured for two samples, and the mean oxidation numbers of niobium in them are deduced to be +4.66 and +4.88. The cell constants of these samples are a = 8.0830(4) and 8.0705(2) Å, respectively. As the mean oxidation number of niobium increases, the color of the compound varies from brown to gray. When the compound is heated in oxygen, it changes into the known white niobium pyrophosphate, in which all niobium is in the +5 oxidation state. Rietveld refinements indicate that niobium pyrophosphates have defects in the phosphorus sites. The topotactic extraction of phosphorus atoms in the reaction with oxygen was confirmed by the analysis of phosphorus oxide generated during the reaction.

INTRODUCTION

There are many pyrophosphates of tetravalent cations (MP_2O_7) with the ZrP_2O_7 structure (M = Ti, Zr, Hf, Mo, W, Re, Si, Ge, Sn, Pb, Ce, Th, U, Np, and Pu) (1–15). The structure can be described as a NaCl-like arrangement of cations and pyrophosphate ions ($P_2O_7^{4-}$) and belongs to the cubic system ($Pa\bar{3}$, No. 205). The range of the cation that can be accommodated in the structure is very wide from the small Si^{4+} cation to the large Th^{4+} cation, which indicates a very large flexibility of the structure. It is noticeable that most of the compounds of this structure have a cubic superstructure with a tripled cell parameter. The superstructure has been observed in the compounds of Zr, Ti, Si, Ge, U, Sn, Pb, Hf, Th, Ce, and Re (2–4, 8, 14, 15).

In the niobium–pyrophosphate system, a compound, which we will call "white niobium pyrophosphate," has been reported (16–19). Its X-ray powder pattern is very similar to the patterns of the ZrP_2O_7-type compounds, but it cannot have the complete ZrP_2O_7 structure, because its white color indicates the niobium in it is pentavalent. Therefore, the compound has been assumed to contain excess oxygen atoms in the ZrP_2O_7 structure and to have the composition of $Nb_2P_4O_{15}$ ($NbO_{1/2}P_2O_7$) (16–18). However, the site of the excess oxygen atoms has not been specified.

Recently Oyetola *et al.* determined the structure of white tantalum(V) pyrophosphate by the single crystal X-ray analysis. It has the ZrP_2O_7-type structure, but contains vacancies in both tantalum and phosphorus sites (19). Owing to these defects, the compound with the ZrP_2O_7 structure can contain tantalum in the pentavalent state. They suggested similar vacancies exist in "white niobium pyrophosphate."

In all previous studies of niobium pyrophosphate, niobium was pentavalent. In the present work, we have prepared a reduced phase of niobium pyrophosphate having the ZrP_2O_7-type structure and studied its nonstoichiometry and the structural change with topotactic oxidation of niobium ions.

EXPERIMENTAL

Starting Material

For the preparation of niobium phosphates, niobium pentaoxide (Nb_2O_5) or hydrated niobium(V) oxides had been commonly used as the starting material, but they were not suitable for the preparation of the phosphates of lower oxidation states. We therefore used niobium chloride $Nb_6Cl_{14} \cdot 8H_2O$. This is a molecular cluster compound having an octahedral Nb_6 cluster unit, and the mean oxidation number of the niobium is +2.33. It was prepared according to the published procedure (20, 21) and recrystallized from HCl solution. Chemical analysis was performed by the published method (22): Nb, 46.00% (calc. 46.54%); Cl, 41.25% (calc. 41.44%).

Brown NbP_2O_7

$Nb_6Cl_{14} \cdot 8H_2O$ and 85% H_3PO_4 were mixed in a gold boat in a ratio of P/Nb $\cong$ 2.3, which is a small excess of phosphoric acid. The total amount of the mixture was about 0.8 g. The gold boat was put in a silica-glass tube placed in an electric furnace, and the tube was continu-

0022-4596/95 $12.00

TABLE 1
Magnetic Parameters of Niobium Pyrophosphates[a]

Sample	Magnetism	χ_0/(emu/g)	C/(emu K/g)	Θ/K	μ^2_{exp}	Oxidation number of Nb
Brown	Paramagnetic	3.8×10^{-8}	48.3×10^{-5}	−0.7	1.03	+4.66 (Nb^{4+} 34%, Nb^{5+} 66%)
Gray	Paramagnetic	-2.0×10^{-7}	17.0×10^{-5}	−0.7	0.36	+4.88 (Nb^{4+} 12%, Nb^{5+} 88%)
White	Diamagnetic[b]	—	—	—	—	+5

[a] Parameters are obtained by the least-squares fitting to the equation $\chi_g = \chi_0 + C/(T - \Theta)$.
[b] Gram susceptibility $\chi_g = -2.83(2) \times 10^{-7}$ cgs · emu/g.

ously evacuated during heating with a rotary vacuum pump. The reaction started at 50–90°C. The temperature was slowly raised to 450°C and held at the temperature more than 4 h. Red–brown niobium pyrophosphate (brown NbP_2O_7) was obtained as a single phase. It was stable in air.

The X-ray powder patterns of the brown NbP_2O_7 samples were slightly different depending on the conditions of the preparation, which implied that the compound was nonstoichiometric. Therefore, among many samples prepared, two samples were selected for detailed examination. The first sample (brown (A)) was prepared by heating at 450°C under reduced pressure for 5 hr, and the second (brown (B)) was prepared by heating at 450°C for 30 hr.

Samples prepared at lower temperature or in a shorter time had brighter red color and seemed to have lower mean oxidation numbers of niobium. However, their IR spectra usually indicated that they contain much phosphoric acid. They are completely decomposed by moisture in air within a month to the niobium(V) orthophosphate reported by Chernorukov *et al.* (17). To obtain samples strictly free from phosphoric acid, we had to heat the sample at a temperature higher than 500°C. In such a sample, niobium is in a higher oxidation state, probably due to the oxidation during the preparation by water in phosphoric acid contained in the sample.

Gray NbP_2O_7

After being ground in air, brown NbP_2O_7 was heated at 800°C for 3 hr with evacuation by a rotary vacuum pump. The reddish tinge of brown NbP_2O_7 faded and gray niobium pyrophosphate (gray NbP_2O_7) was obtained as a single phase.

White NbP_2O_7

Brown or gray NbP_2O_7 heated at the temperature higher than 200°C under an oxygen flow yielded a single phase of white NbP_2O_7. This was identified to be the same compound as the previously reported "white niobium pyrophosphate" from its powder pattern and its color. The white NbP_2O_7 showed diamagnetic property (Table 1), as expected from its color.

X-Ray and Electron Diffraction

Powder X-ray diffraction data were collected on a Rigaku Geiger-Flex RAD-1A system using Cu$K\alpha$ radiation with a Ni filter or on a Rigaku Geiger-Flex RAD-C system using counter-side monochromated Cu$K\alpha$ radiation. The data sets for the Rietveld analysis were collected on the latter system in the step scan mode. The Rietveld analysis program used here was a total pattern fit program RIETAN (23). In the Rietveld analyses of niobium pyrophosphate samples, the data in the ranges with additional peaks probably due to the superstructure of a tripled cell parameter are omitted in order to make a background correction of better quality. Electron diffraction study was performed by using finely crushed particles on a Hitachi 500 100-kV electron microscope.

Other Measurements

Magnetic susceptibility measurements were carried out by using a Faraday balance (Institute for Molecular Science) on powder samples fixed with a small amount of paraffin in a silica-glass cell (24). The magnetic data were corrected by using the measured susceptibility of the cell and paraffin. IR and UV spectra were measured at room temperature on powder samples dispersed in KBr disks by a Hitachi I-3000 spectrometer(IR) and a Hitachi U-3500 spectrometer(UV) equipped with a light condenser.

Analysis of Phosphate Ion

The amount of phosphate ion was determined by the molybdenum blue method. The sample solution with ammonium molybdata in 2 *N* sulfuric acid was reduced by hydrazinium sulfate in boiling water. After cooling in cold water, the blue solution was diluted to the adequate volume, and the absorbance of the solution at 830 nm was measured.

RESULTS AND DISCUSSION

Characterization of Reduced NbP_2O_7

X-ray powder diffraction studies have shown that brown NbP_2O_7 has the ZrP_2O_7 structure. The observed

TABLE 2
X-Ray Diffraction Pattern of Brown NbP_2O_7 [a]

h	k	l	d_{calc}	d_{obs}	I_{obs}
1	1	1	4.67	4.68	33.5
2	0	0	4.04	4.05	100.0
2	1	0	3.61	3.62	31.4
2	1	1	3.30	3.31	28.5
2	2	0	2.86	2.86	26.6
3	1	1	2.44	2.44	35.2
2	2	2	2.33	2.34	6.5
2	3	0	2.24	2.25	3.0
4	0	0	2.021	2.023	3.2
4	1	0	1.960	1.962	3.7
3	2	2			
4	1	1	1.905	1.907	2.3
3	3	1	1.854	1.856	11.9
2	4	0	1.807	1.809	18.6
4	2	0			
4	2	1	1.764	1.765	1.3
2	4	1			
4	2	2	1.650	1.650	11.2
3	3	3	1.556	1.557	16.5
5	1	1			
3	4	2	1.501	1.502	0.5
2	5	1	1.476	1.478	0.4
4	4	0	1.429	1.430	4.9
3	5	1	1.366	1.367	4.6
5	3	1			
4	4	2	1.347	1.348	4.5
5	3	2	1.311	1.312	1.4
6	1	1			
6	2	0	1.278	1.279	2.1
2	6	0			
6	2	1	1.262	1.261	1.1
5	3	3	1.232	1.233	2.5
6	2	2	1.219	1.220	1.5

[a] Data are of sample brown (A).

intensities and d values of the brown (B) sample are given in Table 2. All the reflections can be indexed on the cubic crystal system. Its lattice constant is $a = 8.0809$ Å.

The electron diffraction pattern of the a^*–b^* plane of a brown NbP_2O_7 sample is shown in Fig. 1a. It shows a cubic unit cell ($a_0 = 8.08$ Å) with a systematic absence for $hk0$ ($h = 2n + 1$), which unequivocally determines the space group to be $Pa\bar{3}$ (No. 205). Owing to the problem of multiple diffraction, the systematic absence for $0k0$ ($k = 2n + 1$) does not appear in this photograph. Furthermore, in both Figs. 1a and 1b, a superstructure with a tripled cell parameter ($a' = 3a_0$) is observed as in other ZrP_2O_7-type compounds (2–4, 8). The space group of this superstructure is also $Pa\bar{3}$.

The color indicates that the brown NbP_2O_7 contains Nb^{4+} ions. In the UV spectrum shown in Fig. 2a, only one absorption band is observed at 336 nm and ascribed to the $d \rightarrow d$ electron transition of Nb^{4+} ion (d^1). For comparison, the spectrum of the white NbP_2O_7 is also presented in Fig. 2b. It contains only Nb^{5+} ion (d^0), and there is no absorption band in the measured range.

The temperature-dependent gram magnetic susceptibility of the sample brown (B) in the temperature range 4–250 K is presented in Fig. 3a. This compound shows paramagnetic behavior and follows the Curie–Weiss law quite well in this temperature range. The parameters obtained by fitting the data to the equation

$$\chi_g = \chi_0 + C/(T - \Theta) \qquad [1]$$

are given in Table 1. The near-zero Θ (−0.7 K) indicates very weak interaction between niobium ions, and this is consistent with the structure in which the neighboring Nb–Nb distance is as long as 5.71 Å. The mean oxidation number of niobium in the brown NbP_2O_7 is calculated to be +4.66 (Nb^{4+} 34%, Nb^{5+} 66%), where the spin-only magnetic moment 1.73 μ_B is assumed for Nb^{4+} ion.

Judging from the X-ray powder diffraction pattern, gray NbP_2O_7 has the ZrP_2O_7 structure as the brown samples. The magnetic susceptibility of gray NbP_2O_7 also obeys the Curie–Weiss Law (Fig. 3b), and its Curie constant is much smaller than that of brown NbP_2O_7 as given in Table 1. The calculated mean oxidation number of niobium is +4.88 (Nb^{4+} 12%, Nb^{5+} 88%). Therefore, brown and gray NbP_2O_7 are members of a nonstoichiometric phase of the ZrP_2O_7 structure and have different oxidation states of niobium. The lowest end of the oxidation state in this phase may be close or equal to +4, but we have not been able to obtain the sample in pure form due to the difficulty of removing the phosphoric acid, as described under Experimental. The highest end is higher than +4.88 and lower than +5 because "white niobium pyrophosphate" has pseudo-cubic symmetry.

Structural Defects in Niobium Pyrophosphates

As described in the previous section, mean oxidation numbers of niobium in the pyrophosphates are between 4 and 5. Therefore, their stoichiometry cannot be NbP_2O_7, and they must have some defect or insertion of atoms to keep the ZrP_2O_7 structure. Logically three models of the occupational disorder are possible:

1. Excess-oxygen model: Additional oxygen atoms exist somewhere in the cell.

2. Niobium-defect model: Some of the niobium atoms are deficient.

3. Phosphorus-defect model: Some of phosphorus ions are deficient.

The basic structure of niobium pyrophosphates (i.e., ZrP_2O_7 structure) itself does not imply which model is more probable. A half-unit cell of the ZrP_2O_7 structure projected along the a axis is shown in Fig. 4. The arrange-

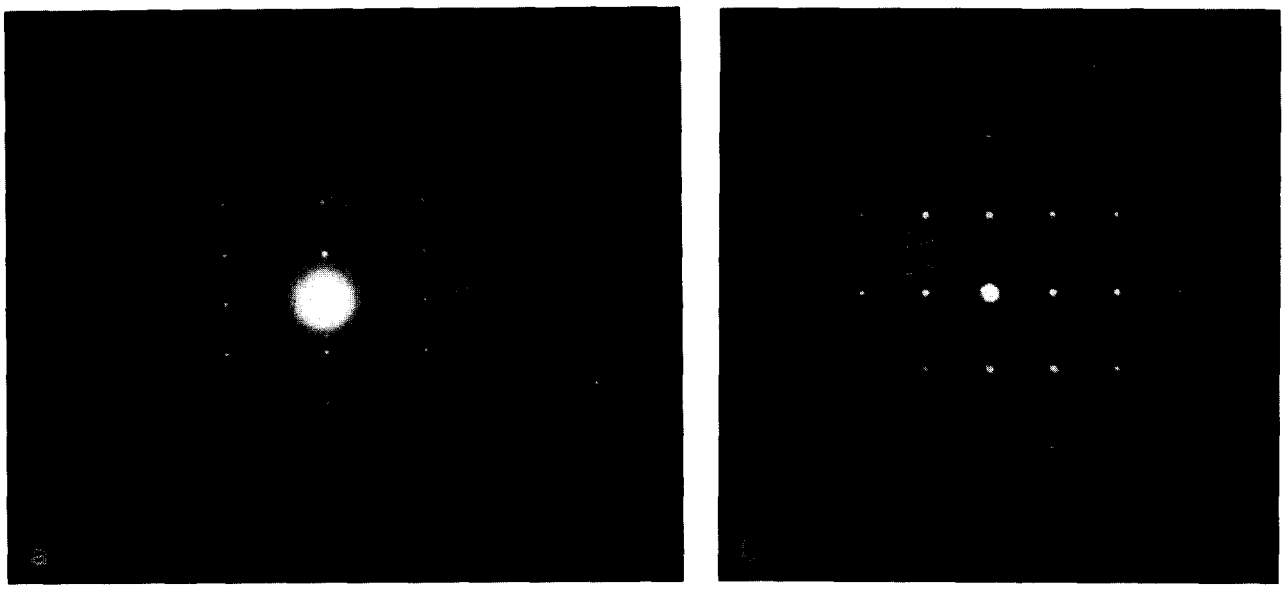

FIG. 1. Electron diffraction patterns of brown NbP_2O_7. Indices are based on the fundamental cubic cell (a = 8.08 Å). (a) Incident beam is parallel to [001]. The systematic absence for $hk0$ ($h = 2n + 1$) is observed. Arrows indicate the superspots indexed with tripled cubic cell parameter ($a' = 3a_0$). (b) Incident beam is parallel to [$\bar{1}$12].

ment of metal cations and pyrophosphate ions is similar to the NaCl structure. Metal atoms are situated at the corners and at the face centers of the unit cell while the centers of the pyrophosphate ions, which are on the oxygen atoms bridging the phosphorus atoms, are located at the middle points of the edges and at the body centers. Phosphorus atoms are located on the threefold axis running along the direction of the body diagonals. Each metal atom is hexacoordinate to form a MO_6 octahedron, connected with six pyrophosphate ions, and each pyrophosphate ion is bound to six metal atoms (Fig. 5). The structure does not seem to have large empty holes to accommodate additional atoms without a large distortion of the cell.

The X-ray powder diffraction data can be used to decide which model is correct. The diffraction patterns of all niobium pyrophosphates are very similar to the pattern expected for $Nb^{IV}P_2O_7$ with the regular ZrP_2O_7 structure (in Fig. 6), but careful examination reveals that relative intensities of the reflections show continuous changes

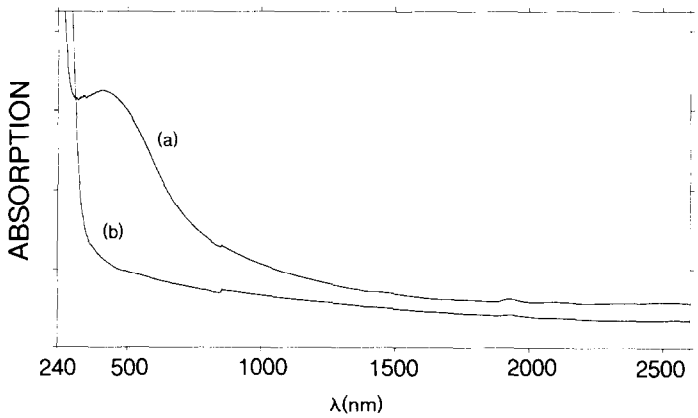

FIG. 2. UV spectrum of a sample of (a) brown NbP_2O_7 and (b) white NbP_2O_7.

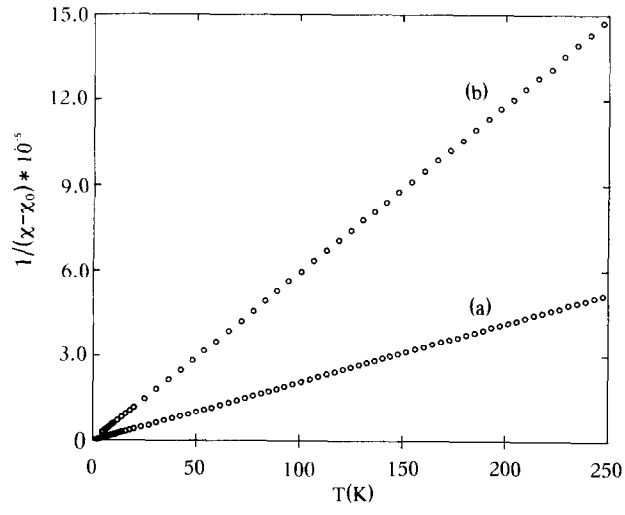

FIG. 3. Temperature dependence of the magnetic susceptibility of (a) brown and (b) gray NbP_2O_7. The ordinate is the value of $(\chi_g - \chi_0)^{-1}$, where χ_0 is determined by the least-squares fitting with Eq. [1]. Both samples obey the Curie–Weiss law.

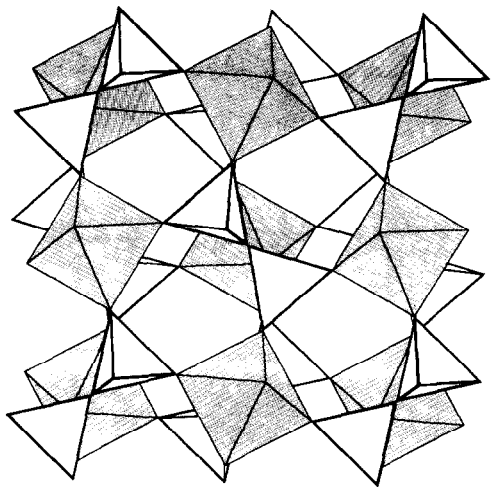

FIG. 4. The crystal structure of NbP_2O_7 projected along a axis. The upper plane is at $z = \frac{1}{2}$ and the bottom at $z = 0$. Shaded octahedra show NbO_6 units, and couples of tetrahedra indicate the pyrophosphate ions ($P_2O_7^{4-}$).

with the oxidation of niobium. Table 3 shows the indices and their relative intensities on four niobium pyrophosphates. Many of the reflections have almost the same relative intensities (e.g., 211, 311, 331), but some reflections change remarkably in their intensities. For instance, the intensity of 111 reflection increases along with the oxidation of niobium. On the other hand, 210 reflection becomes weaker. Such changes of intensity are not ascribable to a preferred orientation because the relative intensity of 222 reflection does not change in spite of the large increase of 111 reflection intensity. These variations seem to reflect a structural change with the oxidation of Nb^{4+} to Nb^{5+}. The sample brown (A) shows the smallest relative intensity value of 111 reflection among the four samples and is considered to be a more reduced phase with the mean oxidation number of Nb close to +4.0.

We now discuss the three models one by one. The excess-oxygen model is the assumption proposed by Haider (16) and Chernorukov (17) for the white NbP_2O_7 to explain why Nb^{5+} cation can exist in the ZrP_2O_7 structure. As described above, however, there is no room for excess oxygen atoms in the ZrP_2O_7 structure. Furthermore, if oxygen atoms are introduced in the structure, the neighboring Nb^{5+} ions should be coordinated by seven oxygen atoms. Nb^{5+} has a small crystallographic radius, and even in the hexacoordinate site, one of Nb–O bonds tends to be longer and forms a square-pyramidal-like structure, e.g., in $NbOPO_4$ (25). We have examined this model by Rietveld analysis by introducing excess oxygen atoms at possible interstitial sites in the structure, but all the results are not consistent with the observed changes the reflection intensities. Therefore, we have concluded that white NbP_2O_7 does not have the "excess-oxygen-inserted" ZrP_2O_7 structure.

The niobium-defect model also does not give reasonable results of the Rietveld analysis. It is very unlikely that in the formation of white NbP_2O_7 a part of niobium is lost under an oxygen flow because there is no volatile chemical species of Nb under the conditions of our synthesis.

Only the phosphorus-defect model gives the changes of the calculated reflection intensities that are consistent with the observation. In this model, the increase of the oxidation number of niobium from Nb^{4+} to Nb^{5+} is caused by the defect of phosphorus atoms. The results of the refinements are presented in Table 4. As an example of the pattern-fitting analysis, the results of the refinement for the gray NbP_2O_7 are illustrated in Fig. 7. The calculated intensities show good agreement with the observed ($R_f = 3.2\%$, $R_{wp} = 14.5\%$).

In the reduced phase, Nb–O distance is 1.93–1.94 Å, and P–O (terminal) bond is 1.48 Å. The angles O–Nb–O are 89° and 91°. The NbO_6 octahedron is almost perfect. Although it is difficult to determine the exact occupational factor of the phosphorus atom from the powder data, Table 4 shows a steady decrease of the factor with the oxidation of the compound. The refined occupational factor of the phosphorus atom is 1.01(4) in the brown (A) sample, 0.96(3) in the brown (B) sample, and 0.905(1) in the gray sample. Then, the mean oxidation numbers of niobium are calculated as follows: 3.9(4) for brown (A), 4.4(3) for brown (B), and 4.95(5) for gray NbP_2O_7. Though

TABLE 3
Relative Intensities of Reflections of Four Niobium Pyrophosphates

h	k	l	Brown (A)	Brown (B)	Gray	White
1	1	1	33.5	34.8	41.2	45.9
2	0	0	100.0	100.0	100.0	100.0
2	1	0	31.4	29.8	28.1	25.4
2	1	1	28.5	27.8	27.2	25.6
2	2	0	26.6	25.1	27.7	28.6
3	1	1	35.2	34.2	36.0	37.8
2	2	2	6.5	5.6	6.4	6.6
2	3	0	3.0	2.2	2.4	2.5
4	0	0	3.2	2.6	3.0	3.4
4	1	0	3.7	3.7	3.9	3.6
3	2	2				
4	1	1	2.3	1.6	2.2	2.6
3	3	1	11.9	11.4	11.1	11.9
2	4	0	18.6	17.8	18.9	19.6
4	2	0				
4	2	1	1.3	1.6	1.7	2.6
2	4	1				
4	2	2	11.2	11.1	14.2	14.9
3	3	3	16.5	17.0	19.6	20.8
5	1	1				

TABLE 4
Results of Rietveld Analysis

Atom	Occupation	x	y	z	B_{eq}
NbP_2O_7, brown (A) sample					
a = 8.0830(4) Å, V = 528.10(8) Å^3, R_F = 1.85%, R_{WP} = 12.02%					
Nb	1	0	0	0	2.4(3)
P	1.01(4)	0.395(2)	= x	= x	3.9(10)
O(1)	1	1/2	1/2	1/2	12.7(24)
O(2)	1	0.2215(9)	0.426(3)	0.445(3)	5.8(9)
NbP_2O_7, brown (B) sample					
a = 8.0807(4) Å, V = 527.65(8) Å^3, R_F = 4.46%, R_{WP} = 17.62%					
Nb	1	0	0	0	2.5(2)
P	0.96(3)	0.394(2)	= x	= x	2.7(8)
O(1)	1	1/2	1/2	1/2	12.2(23)
O(2)	1	0.222(1)	0.429(3)	0.445(3)	5.5(8)
NbP_2O_7, gray sample					
a = 8.0705(2) Å, V = 525.65(4) Å^3, R_F = 3.23%, R_{WP} = 14.52%					
Nb	1	0	0	0	2.36(6)
P	0.905(1)	0.3938(5)	= x	= x	2.0(2)
O(1)	1	1/2	1/2	1/2	11.3(8)
O(2)	1	0.2209(3)	0.424(1)	0.447(1)	5.8(3)
NbP_2O_7, white sample					
a = 8.0896(5) Å, V = 529.39(10) Å^3, R_F = 2.43%, R_{WP} = 16.21%					
Nb	1	0	0	0	1.5(2)
P	0.9	0.393(1)	= x	= x	2.0(5)
O(1)	1	1/2	1/2	1/2	12.6(18)
O(2)	1	0.220(2)	0.431(2)	0.448(2)	5.1(6)

the calculated occupational factors have large standard deviations, they clearly show the tendency of the decrease of the occupation of the phosphorus atom with the increase of the oxidation. The values for the brown (B) and gray NbP_2O_7 show reasonable agreement with those obtained from the magnetic measurements (Table 1). With the decrease of the occupational factor for the P site, the lattice constant also decreases from 8.0830 Å (for brown (A)) to 8.0705 Å (for gray), which seems to be consistent with the phosphorus vacant model.

Another support for the phosphorus-defect model is the density of "white niobium pyrophosphate." Haider reported the density of the white NbP_2O_7 to be D_{obs} = 3.238 g/cm^3 at 25°C, which was much smaller than the value D_{calc} = 3.462 g/cm^3 calculated from the formula $Nb_2O(P_2O_7)_2$ ($NbP_2O_{7.5}$) (16). In our model, however, the composition of the white NbP_2O_7 is $NbP_{1.8}O_7$. Using this formula, we get D_{calc} = 3.283 g/cm^3, which is in good agreement with the observed value.

Topotactic Oxidation of Niobium Pyrophosphates

As described under Experimental, the oxidation of brown NbP_2O_7 yields gray NbP_2O_7 at the first stage, and further oxidation makes white NbP_2O_7. In this reaction,

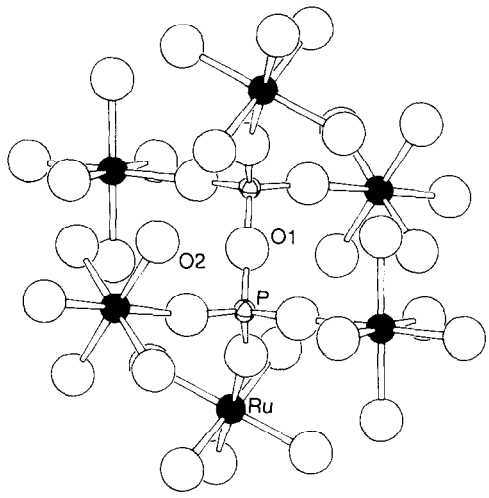

FIG. 5. The linkage of pyrophosphate ion and NbO_6 octahedra. Open and black circles indicate O and Nb atoms, respectively. Small hatched circles show P atoms.

the niobium atoms are oxidized, and the phosphorus atoms are gradually removed without the destruction of the basic structure. Therefore, this series of reaction is an example of topotactic oxidation.

To prove directly the phosphorus removal during this topotactic oxidation, we have quantitatively analyzed the phosphorus pentaoxide generated by the reaction by the following method. Brown NbP_2O_7 samples were put in a gold boat and heated in a Pyrex tube under an oxygen flow at 500°C for 1 day. During the reaction, all the gas coming out from the reaction tube was passed through an aqueous ammonia solution (50 ml H_2O–1 ml NH_3 aq). After the reaction, the complete conversion of brown NbP_2O_7 to white NbP_2O_7 was confirmed by the X-ray

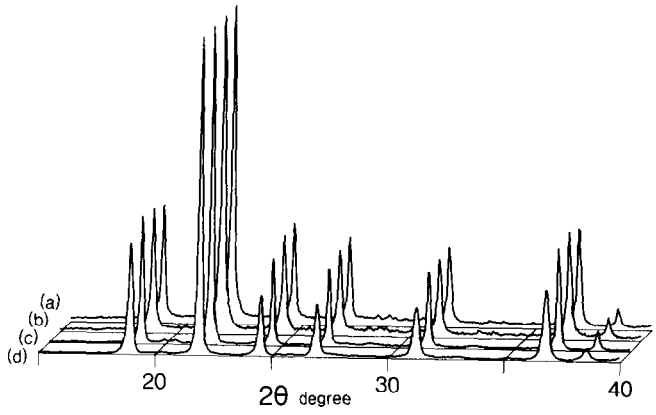

FIG. 6. The X-ray powder diffraction patterns of the various NbP_2O_7 samples. The intensities are normalized so that the strongest peaks have the same height. Integrated intensities are listed in Table 3. (a) Brown (A), (b) brown (B), (c) gray NbP_2O_7, and (d) white NbP_2O_7.

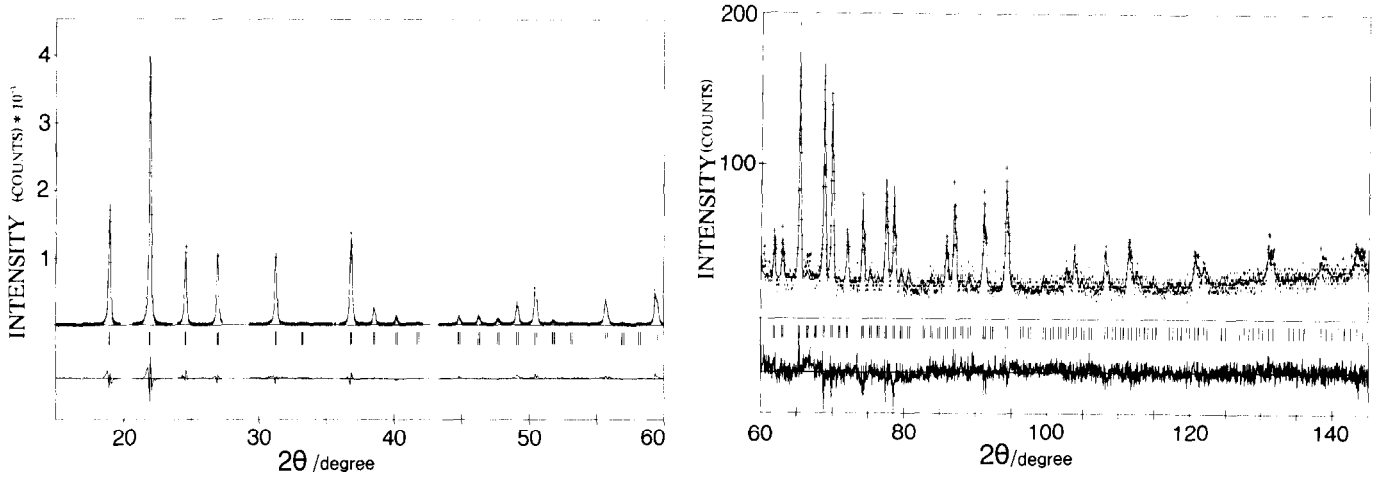

FIG. 7. The result of the Rietveld analysis of gray NbP_2O_7. Cross marks represent observed intensities, the solid line represents calculated intensities, vertical lines show the reflection positions, and the solid line at the bottom of the figure indicates the difference between the observed and calculated intensities.

powder analysis. The phosphorus oxide condensed on the wall of the reaction tube was washed with water and the washings were added to the ammonia solution in the trap. The total amount of phosphate in this solution was determined by the method mentioned in the experimental part. We performed analysis using three samples whose preparative conditions were all different in the reaction temperature and in the mixing ratio of $Nb_6Cl_{14} \cdot 8H_2O$ and phosphoric acid. The results are listed in Table 5.

If the oxidation state of Nb in brown NbP_2O_7 is +4.66, which is derived from the magnetic susceptibility measurement of the sample brown (B) (Table 2), the weight ratio of the extracted phosphorus to the sample will be 0.0080. The analyses of three samples gave 0.0052–0.0060. One of the reasons why the observed values are a little lower than the calculated value is the loss of phosphate ions in all the analytical processes. It is especially difficult to trap completely all phosphorous pentaoxide in the ammonia solution. Another reason is the deviation of the mean oxidation state of niobium among the samples. Because the amount of extracted phosphorus is very small, the samples for this analysis must be completely free from adsorbed phosphoric acid. Therefore, we have heated the samples with evacuation at higher temperature as shown in Table 5, and the samples inevitably had a higher mean oxidation number of niobium, as described under Experimental. The results in Table 5 are consistent with the phosphorus-defect model.

Structure of White NbP_2O_7

Though brown NbP_2O_7 has the superstructure of a tripled cell "white niobium pyrophosphate" has been reported to have no superstructure (19). We have confirmed the loss of the superstructure in white NbP_2O_7 by the electron diffraction. The diffraction pattern in Fig. 8 shows the a^*–b^* plane just as in the photograph of the brown NbP_2O_7 in Fig. 1a. The superspots with a tripled cell parameter are no longer observed in Fig. 8.

Another crystallographic feature of "white niobium pyrophosphate" is its pseudo-cubic symmetry observed with powder diffraction (16) and with the X-ray analysis of twined crystals (19). Larger widths of powder diffraction peaks of white NbP_2O_7 in Fig. 4d may be partly due to this lowering of the symmetry. However, the widths indicate that the deviation from the cubic symmetry is very small, and we performed the Rietveld analysis assuming the cubic symmetry for white NbP_2O_7. In the refinement, the occupational factor of P was fixed to 0.9 because the oxidation number of niobium is +5. The results are given in Table 4. The refined lattice constant a = 8.0896(5) Å is longer than previous studies (8.066 Å (17–19) and 8.073 Å

TABLE 5
Results of Chemical Analysis of Extracted Phosphorus

Sample preparation		Sample weight[c]	Extracted P[d]	
P/Nb[a]	Temperature[b] (°C)	(w/mg)	(p/mg)	p/w
2.32	700	166.7	0.863	0.0052
2.56	600	145.4	0.876	0.0060
2.40	500	136.7	0.812	0.0059

[a] Molar ratio of P/Nb in sample preparation.
[b] Temperature of the sample preparation.
[c] Weight of the sample used for analysis.
[d] Weight of the extracted phosphorus analyzed as phosphate ion.

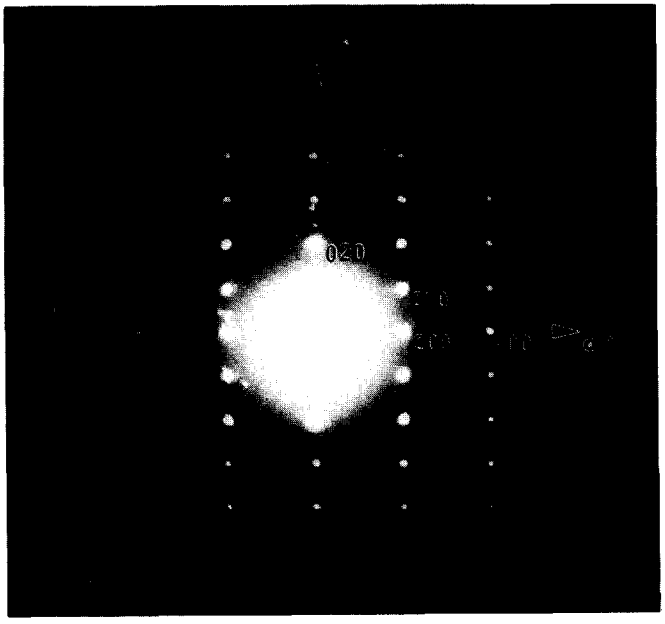

FIG. 8. Electron diffraction patterns of white NbP_2O_7. Incident beams are parallel to [001]. No superspot is observed.

(16)). The reason may be that the crystallinity of our white NbP_2O_7 is not as good as other "white niobium pyrophosphates" prepared directly from Nb^{5+} compounds in previous studies.

The IR Spectra

The IR spectrum of white NbP_2O_7 was reported by Chernorukov *et al.* (17). The spectral pattern is unique and very different from those of other ZrP_2O_7-type compounds (5, 26). The change of IR spectrum with the oxidation of niobium is presented in Figs. 9b–9d. The absorption band around 740 cm^{-1} is always observed in these spectra, which is assigned to the ν_s(P–O–P) symmetric vibrational mode. The spectrum of brown NbP_2O_7 closely resembles spectra of other ZrP_2O_7-type compounds. As the mean oxidation number of niobium increases with the phosphorus defect, the IR pattern becomes more complicated. The fine structures observed in white NbP_2O_7 spectrum suggests the distortion of the $P_2O_7^{4-}$ anion from higher symmetry.

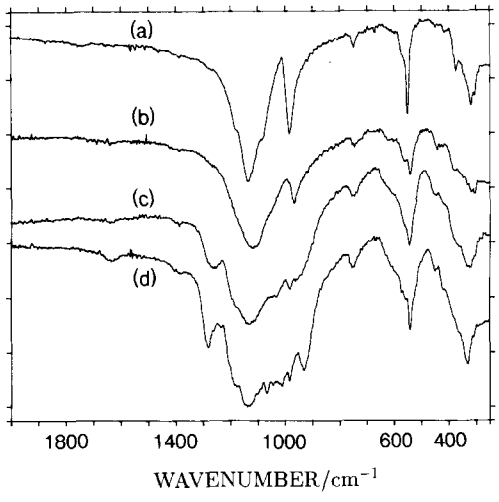

FIG. 9. The change of IR spectra of NbP_2O_7 with the increase of the mean oxidation number of niobium. (a) ZrP_2O_7, (b) brown NbP_2O_7, (c) gray NbP_2O_7, and (d) white NbP_2O_7.

CONCLUSION

Reduced niobium pyrophosphate is a nonstoichiometric compound with defects in the phosphorus site. The number of the defects increases with the oxidation state of niobium. When the number of phosphorus vacancies is not very large, the cubic $Pa\bar{3}$ structure can be held (gray NbP_2O_7). However, when all niobium ions are oxidized to Nb^{5+}, the stress caused by the phosphorus defects induces the distortion of the crystal structure to the pseudo-cubic symmetry.

ACKNOWLEDGMENTS

We are grateful to Professor T. Iwamoto, Dr. Yuge, and Mr. Soma of the University of Tokyo for the powder X-ray diffraction measurements. We thank Mr. Sakai of Institute for Molecular Science for his help in the magnetic measurements. We thank Dr. M. Onoda and Dr. M. Ishii of National Institute for Research in Inorganic Materials (NIRIM) for the electron diffraction measurements and useful discussion. We thank Dr. F. Izumi of NIRIM for his program RIETAN. We thank Dr. Ichikuni of Chiba University for useful discussions about the local structure of NbP_2O_7.

REFERENCES

1. G. R. Levi and G. Peyronel, *Z. Kristallogr.* **92,** 190 (1935).
2. H. Völlenkle, A. Wittmann, and H. Nowotny, *Monatsh. Chem.* **94,** 956 (1963).
3. L.-O. Hagman and P. Kierkegaard, *Acta Chem. Scand.* **23,** 327 (1969).
4. M. Chaunac, *Bull. Soc. Chim. Fr.* **1971,** 424 (1971).
5. C.-H. Huang, O. Knop, D. A. Othen, F. W. D. Woodhams, and R. A. Howie, *Can. J. Chem.* **53,** 79 (1975).
6. D. G. Peyronel, *Z. Kristallogr. A* **94,** 311 (1936).
7. N. Kinomura, M. Hirose, N. Kumada, and F. Muto, *Mater. Res. Bull.* **20,** 379 (1982).
8. E. Banks and R. Sacks, *Mater. Res. Bull.* **17,** 1053 (1982).
9. F. Liebau, G. Bissert, and K. Köppen, *Z. Anorg. Allg. Chem.* **359,** 113 (1968).
10. C. W. Bjorklund, *J. Am. Chem. Soc.* **79,** 6347 (1958).
11. Z. S. Teweldemedhin, K. V. Ramanujachary, and M. Greenblatt, *Mater. Res. Bull.* **28,** 427 (1993).
12. A. Burdese and M. L. Borlera, *Ricerca. Sci.* **30,** 1343 (1960).
13. F. Nectoux and A. Tabuteau, *Radiochem. Radioanal. Lett.* **49,** 43 (1981).

14. E. Tillmanns, W. Gebert, and W. H. Baur, *J. Solid State Chem.* **7,** 69 (1973).
15. A. E. Mal'shikov and I. A. Bondar', *Inorg. Mater.* **25,** 829 (1989).
16. S. Z. Haider, *Proc. Pakistan Acad. Sci.* **1,** 19 (1964).
17. N. G. Chernorukov, N. P. Egorov, and V. F. Kutsepin, *Russ. J. Inorg. Chem.* **24,** 978 (1979).
18. E. M. Levin and R. S. Roth, *J. Solid State Chem.* **2,** 250 (1970).
19. S. Oyetola, A. Verbaere, D. Guyomard, M. P. Crosnier, Y. Piffard, and M. Tournoux, *Eur. J. Solid State Inorg. Chem* **28,** 23 (1991).
20. G. Brauer and A. Simon, *in* "Handbuch der Präparativen Anorganishen Chemie," 3rd ed., Vol. 3, pp. 1444–1445. Enke, Stuttgart, 1981.
21. F. W. Koknat, J. A. Parsons, and A. Vongvusharintra, *Inorg. Chem.* **13,** 1699 (1974).
22. H. Schäfer and K.-D. Dohmann, *Z. Anorg. Allg. Chem.* **300,** 1 (1959).
23. F. Izumi, *in* "The Rietveld Method" (R. A. Young, Ed.), Chap. 13. Oxford Univ. Press, London, 1993.
24. K. Kimura and S. Bandow, *Kotai Buturi* **19,** 467 (1984). [in Japanese]
25. J. M. Longon and P. Kierkegaard *Acta Chem. Scand.* **20,** 72 (1966).
26. R. Pascard, M. Chaunac, and E. Grison, *Bull. Soc. Chim. Fr.* 429 (1971).